

INSTANTANEOUS NON-ACTIVE POWER APPROACH FOR AIRGAP ECCENTRICITY FAULT DIAGNOSIS IN THREE-PHASE INDUCTION MOTORS

M'hamed DRIF, A. J. Marques CARDOSO

University of Coimbra, FCTUC/IT; Department of Electrical and Computer Engineering
Pólo II - Pinhal de Marrocos; P - 3030-290 Coimbra; Portugal
Tel/Fax: + 351 239 796232/796247, E-mail: med_drif@co.it.pt, ajmcardoso@ieee.org

ABSTRACT

This paper firstly presents a modelling and simulation study concerning the occurrence of airgap eccentricity in three-phase induction motors. For that purpose, the winding function approach is considered. Then, the instantaneous non-active power signature analysis is used as a new tool for the detection of mixed airgap eccentricity condition in operating three-phase squirrel cage induction motors. Simulation and experimental results are presented to illustrate the merits of the proposed approach.

Keywords: induction motor, fault diagnosis, non-active power signature analysis, mixed airgap eccentricity, winding function, fault severity factor.

1. INTRODUCTION

Rotating electrical machines play a very important role in the world's industrial life. Faults and failures of critical electromechanical parts can indeed lead to excessive downtimes and generate many costs in reduced output, emergency maintenance and lost revenues. This is why there is a strong industrial demand for reliable and safe operation of these machines and also why industry is interested in adopting monitoring and diagnostic techniques to assess and evaluate electrical machines condition.

One of the faults that may occur in three-phase induction motors is airgap eccentricity [1][2]. It constitutes a major portion of the faults related to induction motors. Almost all mechanical faults lead to this condition, such as faulty bearings, shaft and coupling. These faults result in the displacement of the axis of symmetry or the rotation axis of the rotor. Machine eccentricity is the condition of unequal airgap that exists between the stator and the rotor. Therefore, existing asymmetry between stator and rotor cause other faults in motors. Furthermore, if these faults have not been diagnosed and prevented, the rotor may touch the stator and result in irreparable damage of machines [3].

There are many works dealing with the analysis of the performance of induction motors under eccentricity conditions [4-20]. The Winding Function Approach (WFA) is a useful method for modeling an induction motor under these conditions which accounts for the space harmonics in the machine. Multiple coupled circuit model [1][4-8] enables the dynamic modeling of induction motors with both arbitrary winding layout and/or unbalanced operating conditions. Hence, this model has found application in the analysis of asymmetrical fault conditions in machines such as rotor failures, stator winding faults, or airgap eccentricity [7][8].

Various fault diagnosis techniques have been proposed for airgap eccentricity detection and diagnosis in three-phase induction motors. Some detection techniques evaluate the measured line current of the induction machine. If they are based on the analysis of the Fourier

spectrum of a line current [3-10], they are called motor current signature analysis (MCSA) techniques. From the machine line currents, Park's vector (a space phasor) can also be derived. This vector can be utilized for diagnosing airgap eccentricities [11-13]. Fault-specific signals are also present in the electromagnetic flux which can be measured by coils sensing the axial leakage flux [2][3][14]. Instantaneous power signature analysis is also used. The single-phase instantaneous power was proposed for the diagnosis of mixed rotor faults [15].

Recently, this technique was proposed by the authors for the detection of mixed eccentricity in squirrel cage induction motors, where both simulation and experimental results demonstrated the effectiveness of this approach [16-17]. The partial power as well as the total instantaneous power can be used for the detection of such faults. The complex apparent power was also proposed for the detection and diagnosis of airgap eccentricity condition [18].

In this study, the signature analysis of the non-active power is used, as a new approach for the detection of airgap eccentricity in operating three-phase induction motors, where the application of the imaginary power spectrum for such fault is introduced. It is shown by simulated and experimental results on squirrel cage induction motors that the amount of information carried by this new tool is high and useful for the detection of mixed eccentricity condition.

2. AIRGAP ECCENTRICITY

2.1. Static and dynamic airgap eccentricity

Airgap eccentricity takes two forms: static and dynamic eccentricities. Static eccentricity is characterized by a displacement of the axis of rotation where the position of the minimal airgap length is fixed in space. It can be caused by the stator ovality or by the incorrect positioning of the rotor or stator at the commissioning stage. Since the rotor is not centered within the stator bore, the field distribution in the airgap is no longer symmetrical. The nonuniform airgap gives rise to a radial force of electromagnetic origin, which acts in the

direction of minimum airgap. Therefore, it is called unbalanced magnetic pull (UMP). However, static eccentricity may cause dynamic eccentricity, too [9]. The latter means that the rotor is not rotating on its own axis. In this case, the center of the rotor is not at the center of the rotation and the minimum airgap rotates with the rotor. This kind of eccentricity may be caused by a bent shaft, mechanical resonances, bearing wear or misalignment or even static eccentricity as mentioned above. Therefore, the nonuniform airgap of a certain spatial position is sinusoidally modulated and results in an asymmetric magnetic field, too. This, accordingly, gives rise to a revolving UMP [9][10].

Airgap eccentricity in induction machines causes characteristic harmonic components in electrical, electromagnetic, and mechanical quantities. Therefore, either mechanical quantities such as vibrations or torque oscillations or electrical quantities such as currents or instantaneous power can be analyzed to detect eccentricity conditions [15-20].

In squirrel cage induction motors with airgap eccentricity, characteristic components appear in the stator current spectrum at frequencies given by [4-7][9][10]:

$$f_{ec,i,Hf} = f \left\{ (kR \pm n_d) \frac{(1-s)}{p} \pm v \right\} \quad (1)$$

where:

- f stator supply frequency;
- k an integer;
- R number of rotor bars;
- n_d eccentricity order ($n_d = 0$ for static eccentricity; $n_d = 1, 2, 3, \dots$ for dynamic eccentricity);
- s motor slip;
- v order of the stator time harmonics (1, 3, 5...);
- p number of pole pairs.

Results reported in [9] show that it was inconclusive to identify static or dynamic eccentricity using (1), since a high degree of static eccentricity also produces dynamic eccentricity components. Moreover, the harmonics as described by (1) are not present in the motor for all combinations of p and R [6].

2.2. Mixed airgap eccentricity

In reality, static and dynamic eccentricities tend to coexist. Ideal centric conditions can never be assumed. Therefore, an inherent grade of eccentricity is implied for any real machine, even in newly manufactured ones due to manufacturing and assembly method [10][19]. The combined static and dynamic eccentricity is called mixed eccentricity [9][10][19]. In this condition, both rotor and rotation axes are displaced with respect to the stator one, which results in more complicated geometry condition of the motor compared to the two other cases for its modelling.

It has been shown that sideband components of the slot frequencies in the stator line current given by (1) can be identified [10][19]. However, the exact number of rotor bars has to be known. When static eccentricity is present,

low-frequency components also appear in the current spectrum, which can be given by [4-7][10][19]:

$$f_{ec,i,Lf} = f \pm mf_r = f \left\{ 1 \pm m \frac{(1-s)}{p} \right\} \quad (2)$$

where f_r is the rotational frequency of the machine and m is an integer.

In practice, static and dynamic eccentricities always appear simultaneously. The experimental results presented in [9] show that the current components at frequencies given by (2) are due to the combination of static and dynamic eccentricity (mixed eccentricity).

Apparently, the actual location of those components is a function of the number of pole pairs and slip. The interaction of those harmonics with the mainly sinusoidal supply voltage causes eccentricity specific harmonics in the power and torque spectrum, which appear at the following disturbance frequency [15-19]:

$$f_{ec,p} = mf(1-s)/p = mf_r \quad (3)$$

In the following section, a comprehensive theoretical analysis of mixed eccentricity fault characterization of the induction motor non-active power is presented.

3. ECCENTRICITY CHARACTERISTICS IN THE NON-ACTIVE POWER SIGNATURE ANALYSIS

Many definitions have been formulated to characterize non-active power for nonsinusoidal waveforms in electrical systems, and no single, universally valid power theory has been adopted as a standard for non-active power. Most of the non-active power theories formulated thus far have had a particular type of compensation in mind, which has influenced the conventions used in the development of the definitions. Because nonsinusoidal loads are expected to continue to proliferate throughout electrical distribution systems, non-active power theories will only grow in importance for applications such as non-active power compensation, harmonic load identification, voltage distortion mitigation, and metering [21]. It can be noticed that non-active power is also used in motor speed estimation and control [22].

In this study, the p-q and Park power theories are investigated in the frequency-domain in order to show the effectiveness of the non-active power for the detection of the airgap eccentricity in induction motors.

3.1. Non-active power of a healthy induction motor

3.1.1. p-q Theory

Based on the p-q theory introduced in 1983 by Akagi *et al.* [23-24], by applying Park's transformation to a three-phase, three-wire system (a-b-c) to change it to a two phase plane (α, β) and an orthogonal reactive axis as shown in Fig. 1, they defined the instantaneous non-active (imaginary) power space vector as:

$$\bar{q} = \bar{v}_\alpha \times \bar{i}_\beta + \bar{v}_\beta \times \bar{i}_\alpha \tag{4}$$

where the instantaneous non-active power is given by:

$$q(t) = v_d i_q - v_q i_d \tag{5}$$

As seen in Fig. 1, this space vector is an imaginary axis vector perpendicular to the (α, β) coordinate real plane and is composed of the sum of the products of voltages and currents in orthogonal axes.

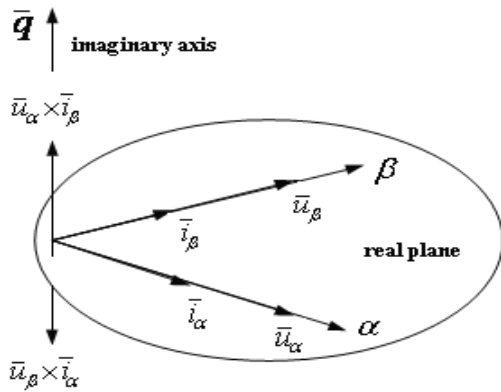


Fig. 1 Instantaneous space vectors of voltage and current of p-q theory [21].

3.1.2. Park power

Using Akagi's Park transformation of phase voltages and currents, Ferrero *et al.* [25-26] defined their instantaneous non-active power differently, which enabled them to generalize their theory based on power definitions. Instead of an (α, β) real plane with an orthogonal imaginary axis q , they used a direct-quadrature (d-q) plane. In a three phase system, they transformed instantaneous voltage and currents to Park vectors (d-q only, without zero sequence) of voltages $\bar{v}(t)$ and currents $\bar{i}(t)$ just as Akagi did and then defined the Park instantaneous complex power as:

$$\bar{s}(t)_p = \bar{v}(t) \cdot \bar{i}^*(t) = (v_d + jv_q)(i_d - ji_q) \tag{6}$$

$$\bar{s}(t)_p = (v_d i_d + v_q i_q) + j(v_q i_d - v_d i_q) \tag{7}$$

They defined the Park imaginary power as:

$$q_p(t) = \text{Im}[\bar{s}(t)_p] = v_q i_d - v_d i_q \tag{8}$$

The only difference between Ferrero's approach and Akagi's approach is that the Park imaginary power (instantaneous non-active power) defined by Ferrero is a characteristic quantity of the three-phase system whereas Akagi's instantaneous imaginary power is not [21].

In case of sinusoidal and symmetrical voltage system, the instantaneous imaginary power $|\bar{q}|$ is equal to the conventional reactive power [21].

While the stator current spectrum of the healthy motor has only a fundamental component at the frequency, f , the spectrum of the imaginary power contains only a dc component.

3.2. Non-active power of an eccentric induction motor

When eccentricity takes place in an induction motor, the stator current, $i_{L, ecc}(t)$ is given by [15-18]:

$$i_{ecc}(t) = I_M \cos[(2\pi f)t - \phi] + \sum_{n=1}^{\infty} \{ I_{ec,m1} \cos[2\pi(f - mf_r)t - \alpha_{m1}] + I_{ec,m2} \cos[2\pi(f + mf_r)t - \alpha_{m2}] \} \tag{9}$$

where $I_{ec,m1}$ and α_{m1} are the amplitude of the current component at a frequency $(f - mf_r)$ and its initial phase angle; $I_{ec,m2}$ and α_{m2} are the amplitude of the current component at a frequency $(f + mf_r)$ and its initial phase angle. Clearly, in the current spectrum, two sideband components will appear around the fundamental component at frequencies $(f - f_r)$ and $(f + f_r)$ [15-19].

In this case, the non-active power is then given by:

$$q(t) = q_0(t) + \Delta_{ecc} q(t) \tag{10}$$

where $q_0(t)$ is the healthy motor imaginary power and $\Delta_{ecc} q(t)$ is the imaginary power pulsation due to the eccentricity fault at the disturbance frequency f_r .

The spectrum of the non-active power in the case of an eccentric machine contains the dc component and a harmonic component at the disturbance frequency f_r . The latter additional component at the modulation frequency, subsequently called characteristic component, provides an extra piece of diagnostic information about the condition of the machine.

4. SIMULATION RESULTS

A mathematical model has been developed in order to investigate mixed eccentricities. This is a multi-harmonic model that also evaluates higher harmonics [1][4-8]. By means of this model, typical harmonic eccentricity components can be predicted. The respective harmonics arise in the machine currents [4-6], torque [19], and power [15-19].

The analysis is based on the winding function and the coupled-circuits theories. To study the performance of squirrel cage induction motors with mixed eccentricity, a mesh model of the rotor is selected [7][8]. The rotor is described in the terms of loops. Rotor loop currents are defined as the currents flowing in loops comprising two adjacent rotor bars and the portions of end ring joining them. Each rotor bar and end ring segment are characterized by a resistance and inductance. For a three-phase squirrel cage induction motor with N_b bars, N_b+3 windings couple with each other through the airgap flux.

The mathematical model of the squirrel cage induction motor is given by the following differential equations system:

$$\begin{cases} \frac{d}{dt}[I] = -[L]^{-1} \left[[R] + \omega_m \frac{d[L]}{d\theta_m} \right] [I] + [L]^{-1} [V] \\ \frac{d\omega_m}{dt} = \frac{1}{2J} [I]^T \left\{ \frac{d[L]}{d\theta_m} \right\} [I] - \frac{T_L}{J} \\ \frac{d\theta_m}{dt} = \omega_m \end{cases} \quad (11)$$

All of the relevant inductances for the induction motor can be calculated using the WFA given in [1][4-8]. The approach assumes no symmetry in the placement of any motor coil in the slots. According to the winding function theory, the mutual inductance between any two windings "i" and "j" in any electric machine can be computed by:

$$L_{ij}(\theta_r) = \mu_0 \ell \int_0^{2\pi} r(\theta_r, \phi) g_e^{-1}(\theta_r, \phi) n_i(\theta_r, \phi) N_j(\theta_r, \phi) d\phi \quad (12)$$

where θ_r is the angular position of the rotor with respect to some stator reference, ϕ is a particular position along the stator inner surface, $g_e^{-1}(\theta_r, \phi)$ is termed the inverse effective airgap function, ℓ is the length of the stack, and r is the average radius of the airgap. The term $n_i(\theta_r, \phi)$ is the winding distribution of the winding i , and $N_j(\theta_r, \phi)$ is called the winding function and represents in effect the magneto-motive force (MMF) distribution along the airgap for a unit current flowing in the winding j .

In the presence of mixed eccentricity the airgap can be modeled as [4][8]:

$$g_e(\theta_r, \phi) = g_0 [1 - a_1 \cos(\phi) - a_2 \cos(\phi - \theta_r)] \quad (13)$$

where a_1 and a_2 are the amount of static and dynamic eccentricity, respectively, and g_0 is the average airgap.

The inverse airgap function can then be defined as [4]:

$$g_e^{-1}(\theta_r, \phi) = \frac{1}{g_0 [1 - a_3 \cos(\phi - \theta_r)]} \quad (14)$$

with

$$a_3 = \sqrt{a_1^2 + 2a_1a_2 \cos(\theta_r) + a_2^2} \quad (15)$$

$$\theta_r' = \arctan \left(\frac{a_2 \sin(\theta_r)}{a_1 + a_2 \cos(\theta_r)} \right) \quad (16)$$

The inverse airgap function is approximated as:

$$g_e^{-1}(\theta_r, \phi) = G_0 + G_1 \cos(\phi - \theta_r') \quad (17)$$

where:

$$G_0 = \frac{1}{g_0 \sqrt{1 - a_3^2}} \quad (18)$$

$$G_1 = \frac{2}{g_0 \sqrt{1 - a_3^2}} \left(\frac{1 - \sqrt{1 - a_3^2}}{a_3} \right) \quad (19)$$

All the machine inductances can be calculated in the case of mixed eccentricity using the equation (12).

Further details about the mathematical model of the induction motor using the WFA and about the machine inductances which are dependent on the rotor position in the case of mixed eccentricity are given in [1][4-8].

A fourth order Runge-Kutta numerical integration method is used to solve the first-order differential equations (11).

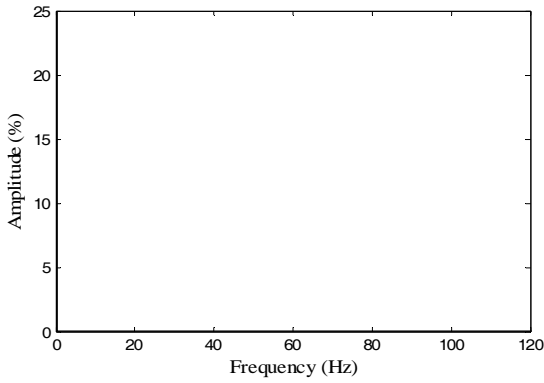
The advantages of the presented technique are confirmed by simulation, on a 50 Hz, 7.5 Hp, 380/220 V, 4-poles, three-phase squirrel cage squirrel cage induction motor, using the aforementioned model. Initially, the healthy motor drives a load with a constant torque. Its non-active power signature is shown in Fig. 2(a). Obviously, only a dc component is present.

When a mixed eccentricity fault condition is introduced (10% of dynamic and 16% of static eccentricities), the motor speed and slip begin oscillating due to the pulsating torque at $f_r = f(1-s)/p = 24.4$ Hz. As a result of this situation, the non-active power signature significantly differs from that of a healthy motor, as shown in Fig. 2(b). In the spectrum of the non-active power modulus, a frequency component appears directly at the frequency of speed oscillation $f_r = 24.4$ Hz, with an amplitude of 2.94%. Also shown are the spectral components corresponding to $m=2$ and some sidebands. When the severity of the fault is increased (10% of dynamic and 66% of static eccentricities), the non-active power signature (Fig. 2(c)) shows that the amplitude of the characteristic frequency at $f_r = 24.4$ Hz also increases to 19.77%, as well as for the others aforementioned spectral components.

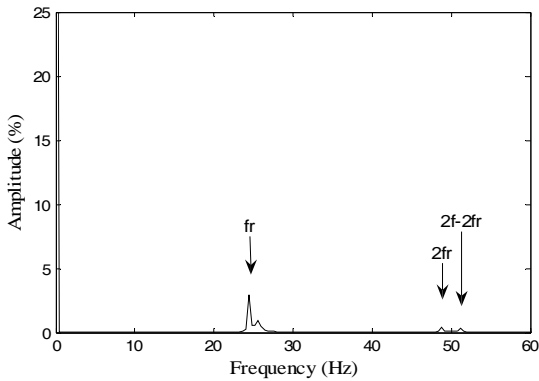
5. EXPERIMENTAL RESULTS

The test motor used in the experimental investigation was a squirrel cage three-phase, 50 Hz, 4-pole, 3 kW, AEG induction machine, type Dd 150/150 - 4 univ, with several rotors of different types, which can be easily interchanged. A separately excited dc generator feeding a variable resistor provided a mechanical load. The diagnostic instrumentation system used basically comprises a microcomputer, supporting a data acquisition board, clip-on current probes, differential voltage probes, and a preconditioning module (Fig. 3). All details of the experimental test rig are given in [11].

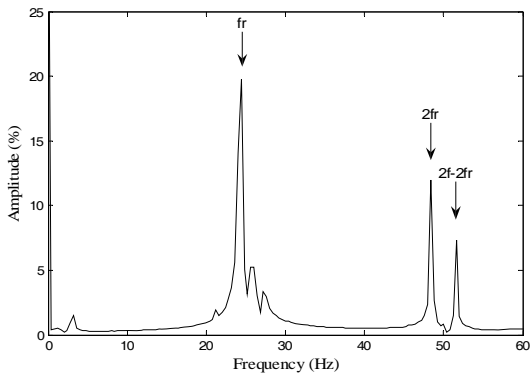
The motor was initially tested without eccentricity. Fig. 4(a) shows the non-active power signature for this case. It is shown that in the absence of fault, the behaviour of the motor is not only characterised by the presence of a dc component as theoretically predicted, but also by the appearance of the previously identified components characteristics of the fault. This is due to the presence of some inherent eccentricities in the tested motor, like as in any other real machine.



(a) - Healthy motor.



(b) - Eccentric motor (DE=10%, SE=16%).



(c) - Eccentric motor (DE=10%, SE=66%).

Fig. 2 Simulation results.

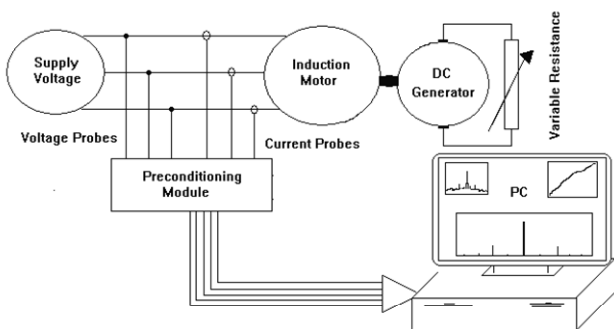
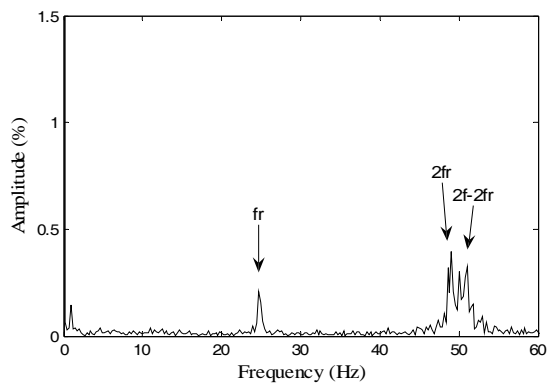


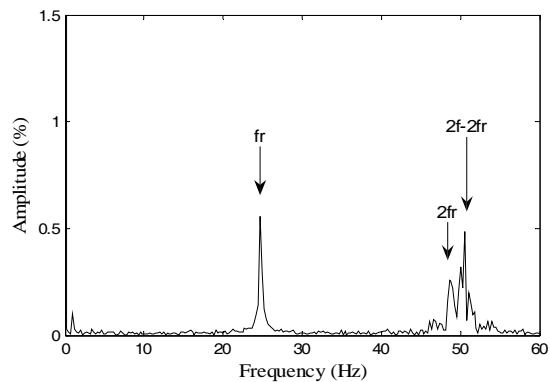
Fig. 3 Synoptic scheme of the induction motor diagnostic system.

The introduction of a 16% static eccentricity level is clearly noticeable in the non-active power signature of Fig. 4(b), by the increased amplitude of the characteristic component at $f_r = f(1-s)/p = 24.66$ Hz. When a static eccentricity level of 66% is introduced in the test motor, the amplitude of the characteristic component, f_r , increases accordingly, as can be seen in Fig. 4(c). It is however interesting to note that the previously identified additional spectral components at $2f_r$ and $2f - 2f_r$, remain almost with the same amplitude despite the increase in the fault severity level. This can be due to the effect of the motor/load inertia

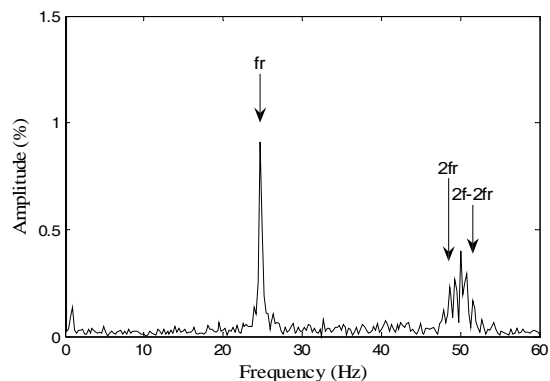
The experimental spectra in Fig. 4, show also the presence of the fundamental component of the supply frequency, f , which is due to the pollution of the voltage system (presence of even harmonics) as shown in Fig. 5.



(a) - Healthy motor



(b) - Eccentric motor (SE=16%).



(c) - Eccentric motor (SE=66%).

Fig. 4 Experimental results.

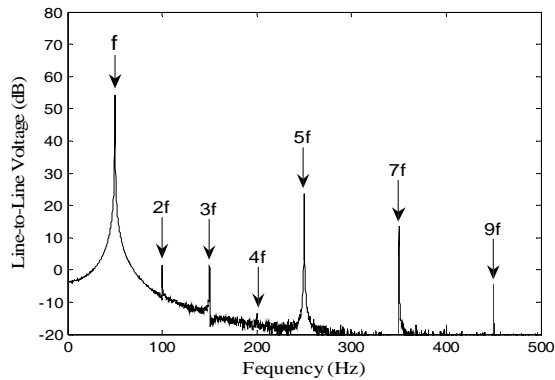


Fig. 5 Line-to-line voltage spectrum (experimental results).

As for the results shown in Figs. 2 and 4, one can notice a difference in the amplitude of the parameters involved, which is due to the fact that motors with different power ratings are used in simulation studies and experimental tests. However the same behavior has been achieved.

In order to show the effectiveness of the proposed approach for the detection of mixed eccentricity condition in induction motors, a normalized severity factor was defined as the ratio of the amplitude of the fault characteristic component, f_r , in the spectrum of instantaneous non-active power of the motor, and the corresponding dc value.

Figs. 6 and 7 show the evolution of the defined fault severity factors for the simulation and experimental results, respectively, under full load conditions. The results show that there is an increase in the value of the normalized fault severity factor with the extension of the fault, making it a good indicator of the machine condition.

6. CONCLUSIONS

This paper introduces a new approach, based on a spectral analysis of the non-active power for detecting the occurrence of airgap eccentricity in operating three-phase induction motors. The experimental and simulated results show that mixed eccentricity condition can be effectively detected by this new technique, whose operating philosophy relies on the behavior of the spectral component at a frequency of $f_r = f(1-s)/p$. This characteristic spectral component of the non-active power appears directly at the frequency of disturbance. This is important in automated diagnostic systems, in which the irrelevant frequency components i.e., those multiples of the supply frequency, are screened out.

It is known that airgap eccentricity fault generates sideband components at frequencies differing from the fundamental in the current spectrum, becoming necessary in some cases to filter out the fundamental component [11]. In contrast, the characteristic component in the spectrum of the non-active power is far apart from the other harmonics and always with an amplitude corresponding to the fault level.

Furthermore, the use of the non-active power for the detection of airgap eccentricity condition provides simultaneous information about the current and voltage,

which can be of paramount importance when in the presence of an unbalanced and polluted supply voltage system.

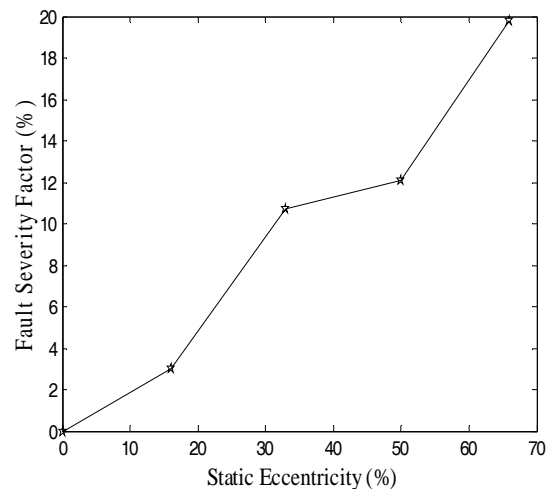


Fig. 6 Instantaneous non-active power fault severity factor (simulation results).

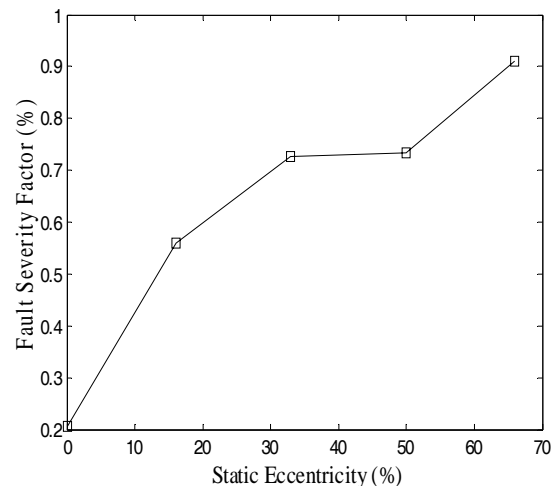


Fig. 7 Instantaneous non-active power fault severity factor (experimental results).

ACKNOWLEDGEMENT

The authors gratefully acknowledge the financial support of the Portuguese Foundation for Science and Technology (FCT) under Project N°. SFRH/BD/17592/2004.

REFERENCES

- [1] Devanneux, V.; Kabbaj, H.; Dagues, B.; Faucher, J.: An accurate model of squirrel cage induction machines under static, dynamic or mixed eccentricity, Proc. IEEE SDEM-PED'01, 2001, pp. 121-126.
- [2] Tavner, P. J.; Penman, J. : Condition monitoring of electrical machines, Res. Studies Press, John Wiley & Sons, 1987.

- [3] Cameron, J. R.; Thomson, W. T.; Dow A. B. : Vibration and current monitoring for detecting airgap eccentricity in large induction motors, IEE Proc., Part B, vol. 133, May 1986, pp. 155-163.
- [4] Nandi, S.; Bharadwaj, R. M.; Toliyat H. A. : Mixed eccentricity in three phase induction machines: Analysis simulation and experiments, Conf. Rec. IEEE-IAS Annu. Meeting, vol. 3, 2002, pp. 1525-1532.
- [5] Nandi, S.; Bharadwaj, R. M.; Toliyat, H. A. : Performance analysis of a three phase induction motor under mixed eccentricity, IEEE Trans. on Energy Conversion, vol. 17, n° 3, Sept. 2002, pp. 392-399.
- [6] Nandi, S.; Ahmed, S.; Toliyat, H. A. : Detection of rotor slot and other eccentricity related harmonics in a three phase induction motor with different rotor cages, IEEE Trans. on Energy Conversion, vol. 16, n° 3, Sept. 2001, pp. 253-260.
- [7] Joksimovic, G. M.; Duvoric, M.; Penman, J.; Arthur N. : Dynamic simulation of dynamic eccentricity in induction machines - Winding Function Approach, IEEE Trans. on Energy Conversion, vol. 15, n° 2, June, 2000, pp. 143-148.
- [8] Toliyat, H. A.; Arefeen, M. S.; Parlos, A. G. : A method for dynamic simulation of air-gap eccentricity in induction machines, IEEE Trans. on Ind. Applic., vol. 32, n° 4, Jul/Aug. 1996, pp. 910-918.
- [9] Thomson, W. T.; Rankin, D.; Dorrell, D. G. : Online current monitoring to diagnose airgap eccentricity in large induction motors – Industrial case histories verify the predictions, IEEE Trans. on Energy Conversion, vol. 14, Dec. 1999, pp. 1372-1378.
- [10] Nandi, S.; Toliyat, H. A.; Li, X. : Condition monitoring and fault diagnosis of electrical motors - A review, IEEE Trans. on Energy Conversion, vol. 20, n° 4, Sept. 2005, pp. 719-729.
- [11] Cardoso, A. J. M.; Saraiva, E. S.; Mateus, M. L.; Ramalho, A. L. : On-line detection of air-gap eccentricity in 3-phase induction motors, by Park's vector approach, IEE 5th Int. Conf. on Elect. Mach. and Drives, London, UK, IEE Conf. Public., n° 341, Sept. 1991, pp. 61-66.
- [12] Cardoso, A. J. M.; Saraiva, E. S. : Computer-aided detection of airgap eccentricity in operating three-phase induction motors by Park's vector approach, IEEE Trans. on Ind. Applic., vol. IA-29, n° 5, Sept/Oct 1993, pp. 897-901.
- [13] Cardoso, A. J. M.; Saraiva, E. S. : Predicting the level of airgap eccentricity in operating three-phase induction motors, by Park's vector approach, Conf. Rec. IEEE-IAS Ann. Meeting, vol. I, Texas, USA, 1992, pp. 132-135.
- [14] Dorrell, D.; Thomson, W.; Roach, S. : Analysis of airgap flux, current and vibration signals as a function of the combination of static and dynamic airgap eccentricity in 3-phase induction machines, Conf. Rec. IEEE-IAS Annu. Meeting, 1995, pp. 563-570.
- [15] Liu, Z.; Yin, X.; Zhang, Z.; Chen, D. : Online rotor mixed fault diagnosis way based on spectrum analysis of instantaneous power in squirrel cage induction motors, IEEE Trans. on Energy Conversion, vol. 19, n° 3, Sept. 2004, pp. 485-490.
- [16] Drif, M.; Cardoso, A. J. M.; Benouzza, N. : Instantaneous power signature analysis for detecting airgap eccentricity in three-phase induction motors, Proc. ICEL' 2005, Oran, Algeria, Nov. 2005, 7 p.
- [17] Drif, M.; Cardoso, A. J. M. : Airgap eccentricity fault diagnosis, in three-phase induction motors, by the instantaneous power signature analysis, 3rd IEE Inter. Conf. on Power Electronics, Machines and Drives, (PEMD 06), 4-6 April 2006, Dublin, Ireland, pp. 349-353.
- [18] Drif, M.; Cardoso, A. J. M. : Airgap eccentricity fault diagnosis, in three-phase induction motors, by the complex apparent power signature analysis, IEEE Trans. on Ind. Elec., vol. 55, n° 3, March 2008, pp. 1404-1410.
- [19] Kral C.; Habetler, T. G.; Harley, R. G. : Detection of mechanical imbalance of induction machines without spectral analysis of time – domain signals, IEEE Trans. on Ind. Applic., vol. 4, n° 4, Jul/Aug 2004, pp. 1101-1106.
- [20] Kral, C.; Pirker, F.; Pascoli, G. : Rotor eccentricity detection of induction machines by means of torque estimation-measurement results, Proc. IEEE SDEMPED'99, 1999, pp. 283-287.
- [21] Tolbert, L. M.; Habetler, T. G. : Comparison of time-based non-active power definitions for active filtering, CIEP, Mexico, 15-19 Oct., 2000, pp. 73-79.
- [22] Betz, R.E.; Summers, T. : Speed estimation for induction machines using imaginary power, IEEE – IAS Annual Meeting Conf., Vol. 1, 12-16 Oct 2003, pp. 117-123.
- [23] Akagi, H.; Kanazawa, Y.; Nabae, A. : Instantaneous reactive power compensators comprising switching devices without energy storage components, IEEE Trans. Ind. Applic., vol. IA-20, n° 3, May 1984.
- [24] Akagi, H.; Nabae, A. : The p-q theory in three-phase systems under non-sinusoidal conditions, ETEP, vol. 3, Jan. 1993, pp. 27-31.
- [25] Ferrero, A.; Superti-Furga, G. : A new approach to the definition of power components in three-phase systems under nonsinusoidal conditions, IEEE Trans. Instrum. Meas., vol. 40, June 1991, pp. 568-577.
- [26] Ferrero, A.; Morando, A. P.; Ottoboni, R.; Superti-Furga, G. : On the meaning of the Park power components in three-phase systems under non-sinusoidal conditions, ETEP, vol. 3, Jan. 1993, pp. 33-43.

Received June 8, 2006, accepted June 10, 2008

BIOGRAPHIES



M'hamed Drif was born in Saida, Algeria, in 1964. He received his Electrical Engineering diploma and Master's degree, in 1989 and 1993 respectively, from the University of Science and Technology of Oran (USTO), Oran, Algeria. Between 1993 and 2004, he was an assistant

Professor in the same University. Since 1996, he is working in the field of fault diagnosis in electrical drives. In 2005, he joined the University of Coimbra, in Portugal, where he is presently working towards his PhD, in the same field. He has authored national and international technical conference and journal papers.



A. J. Marques Cardoso (S'89, A'95, SM'99) was born in Coimbra, Portugal, in 1962. He received the E. E. diploma and the Dr. Eng. degree from the University of Coimbra, Coimbra, Portugal, in 1985 and 1995, respectively. Since 1985, he has been with the University of Coimbra,

where he is currently an Associate Professor in the Department of Electrical and Computer Engineering and Director of the Electrical Machines Laboratory. His teaching interests cover electrical rotating machines, transformers, and maintenance of electro-mechatronic systems and his research interests are focused on condition monitoring and diagnostics of electrical machines and drives. He is the author of a book entitled *Fault Diagnosis in Three-Phase Induction Motors* (Coimbra, Portugal: Coimbra Editora, 1991), (in

Portuguese) and about 200 papers published in technical journals and conference proceedings.

Dr. Marques Cardoso is actively involved in the field of standardization on condition monitoring and diagnostics, both at the national and international level, where he has been acting as a convenor of ISO/TC 108/SC 5 Advisory Group D (Condition Monitoring and Diagnostics of Power Transformers) and ISO/TC 108/SC 5 Working Group 10 (Condition Monitoring and Diagnostics of Electrical Equipment), and also a member of several Working Groups/Balloting Committees of ISO, IEEE and CEN.

He was a member of the Overseas Advisory Panel of *Condition Monitoring and Diagnostic Technology* (a journal published by the British Institute of Non-Destructive Testing between 1990-1993), and he is currently a member of the Editorial Board of the *International Journal of Condition Monitoring & Diagnostic Engineering Management*, published by COMADEM International, UK, an Honorary Member of the International Biographical Centre Advisory Council, Cambridge, England, and also an Honorary Professor of the Albert Schweitzer International University, Geneva, Switzerland.

Dr. Marques Cardoso is a member of the New York Academy of Sciences, the European Power Electronics and Drives Association (EPE), the Electrical Machines and the Industrial Drives Committees of the IEEE Industry Applications Society, the Electrical Machines and the Power Electronics Committees of the IEEE Industrial Electronics Society, the Technical Committee on Diagnostics of the IEEE Power Electronics Society, the Portuguese Federation of Industrial Maintenance (APMI), and a senior member of the Portuguese Engineers Association (ODE). He has been listed in *Who's Who in the World*, *Who's Who in Science and Engineering*, *BEST Europe*, among others.